

β 4 Integrin Amplifies ErbB2 Signaling to Promote Mammary Tumorigenesis

Wenjun Guo,^{1,2,6} Yuliya Pylayeva,^{1,2} Angela Pepe,¹ Toshiaki Yoshioka,^{1,7} William J. Muller,³ Giorgio Inghirami,^{4,5} and Filippo G. Giancotti^{1,*}

¹ Cell Biology Program, Memorial Sloan-Kettering Cancer Center, New York, NY, 10021 USA

² Sloan-Kettering Division, Weill Graduate School of Medical Sciences, Cornell University, New York, NY, 10021 USA

³ Molecular Oncology Group, McGill University, Royal University Hospital, Montreal, Quebec H3A 1A1, Canada

⁴ Department of Pathology and Center for Experimental Research and Medical Studies, University of Torino, 10060 Torino, Italy

⁵ Department of Pathology and NYU Cancer Institute, NYU School of Medicine, New York, NY 10016, USA

⁶ Present address: Whitehead Institute for Biomedical Research, Cambridge, MA 02142, USA.

⁷ Present address: Department of Pathology and Immunity, Akita University School of Medicine, 1-1-1 Hondo, Akita City, Akita 010-8543, Japan.

*Contact: f-giancotti@ski.mskcc.org

DOI 10.1016/j.cell.2006.05.047

SUMMARY

Amplification of the *ErbB2* locus, which encodes a receptor tyrosine kinase, is common in aggressive breast tumors and correlates with poor prognosis. The mechanisms underlying ErbB2-mediated breast carcinoma progression remain incompletely defined. To examine the role of the signaling and cell-adhesion receptor β 4 integrin during ErbB2-mediated tumorigenesis, we introduced a targeted deletion of the β 4 signaling domain into a mouse model of ErbB2-induced mammary carcinoma. Loss of β 4 signaling suppresses mammary tumor onset and invasive growth. Ex vivo studies indicate that β 4 forms a complex with ErbB2 and enhances activation of the transcription factors STAT3 and c-Jun. STAT3 contributes to disruption of epithelial adhesion and polarity, while c-Jun is required for hyperproliferation. Finally, deletion of the β 4 signaling domain enhances the efficacy of ErbB2-targeted therapy. These results indicate that β 4 integrin promotes tumor progression by amplifying ErbB2 signaling and identify β 4 as a potential target for molecular therapy of breast cancer.

INTRODUCTION

Breast cancer is the most common malignancy in women and causes over 400,000 deaths per year (Parkin et al., 2005). About 30% of all breast cancers carry amplifications of the *ErbB2* locus, which encodes the receptor tyrosine kinase (RTK) ErbB2 (Slamon et al., 1987). These tumors have an aggressive behavior, high rates of relapse, and poor prognosis (Berger et al., 1988). In agreement

with the hypothesis that ErbB2 signaling initiates mammary tumorigenesis, the levels of ErbB2 increase at the onset of ductal carcinoma in situ (DCIS) (van de Vijver et al., 1988). Furthermore, dimerization of ErbB2 induces proliferation and suppresses apoptosis in MCF-10A mammary epithelial acini, yielding solid multiacinar structures resembling DCIS (Muthuswamy et al., 2001). Finally, transgenic mice expressing constitutively activated ErbB2 (Neu) in their mammary glands develop invasive ductal carcinomas (Muller et al., 1988), directly implicating ErbB2 signaling in mammary oncogenesis.

Oncogene-induced hyperproliferation and suppression of apoptosis are sufficient to induce luminal filling and expansion of carcinoma in situ in glandular epithelia (Debnath et al., 2002). Progression to invasive carcinoma, however, requires that cancer cells disassemble intercellular junctions, reorientate their cytoskeletons, and finally invade into the interstitial matrix. Certain oncogenic mutations and combinations thereof can cause this gain in motility in vitro, and studies with various cellular models of tumor progression have identified a plethora of putative pathogenic pathways (Thiery, 2002). However, the mechanisms by which *ErbB2* amplifications or other oncogenic lesions promote breast carcinoma progression in vivo remain poorly understood.

Current insight into this problem derives largely from studies on E-cadherin. E-cadherin mediates assembly of adherens junctions and operates to restrain carcinoma invasion. Lobular carcinomas of the breast often exhibit loss-of-function mutations of *E-cadherin* or methylation of its promoter (Cavallaro and Christofori, 2004). Furthermore, they often express elevated levels of the bHLH transcription factor Twist, which silences the expression of E-cadherin as part of its proinvasive epithelial-to-mesenchymal transition (EMT) program (Yang et al., 2004). However, common ductal carcinomas of the breast, including ErbB2-positive tumors, often retain expression of E-cadherin (Gamallo et al., 1993), suggesting that other mechanisms can disrupt epithelial adhesion and polarity in these tumors.

Studies of in vitro models suggest that the $\alpha 6 \beta 4$ integrin—a component of hemidesmosomes—contributes to oncogenesis by sustaining RTK signaling. $\beta 4$ integrin signaling proceeds through Src family kinase (SFK) mediated phosphorylation of the cytoplasmic domain of $\beta 4$, recruitment of Shc, and activation of Ras and PI-3K (Mainiero et al., 1997; Shaw et al., 1997). The RTKs ErbB2, EGF-R, and Met associate with $\alpha 6 \beta 4$, and there is evidence suggesting that they promote invasive signaling through phosphorylation of $\beta 4$ (Falcioni et al., 1997; Mariotti et al., 2001; Trusolino et al., 2001). Accordingly, wild-type, but not signaling-defective, $\beta 4$ causes a gain in invasive ability in a breast carcinoma cell line expressing Met (Shaw et al., 1997). In spite of this body of work, the hypothesis that $\alpha 6 \beta 4$ has a protumorigenic function remains controversial. Expression of wild-type, but not signaling-defective, $\beta 4$ activates p53 and induces cell-cycle arrest and apoptosis in rectal carcinoma cells (Bachelder et al., 1999). Furthermore, antibody blockage of $\alpha 6 \beta 4$ disrupts mammary epithelial polarity and promotes hyperproliferation in 3D Matrigel (Weaver et al., 1997). These complex and apparently contrasting effects of $\alpha 6 \beta 4$ may reflect physiologically distinct roles of this integrin in different cancer cells or intrinsic limitations of these models.

Given the complexity of tumor progression, it is important to use experimental models that closely mimic the evolution of human breast cancer while allowing molecular manipulation. DNA microarray data reveal that the basal-like ductal breast carcinomas and related ErbB2-positive tumors often express high levels of $\beta 4$ (Sorlie et al., 2001). To examine whether $\beta 4$ signaling plays a role in ErbB2-mediated mammary tumorigenesis, we have introduced a targeted deletion of the $\beta 4$ signaling domain in MMTV-*Neu* mice. By combining in vivo analysis with an ex vivo RNAi knockdown/reconstitution approach, we provide evidence that $\beta 4$ combines with ErbB2 and amplifies its signaling ability, enabling mammary tumor progression.

RESULTS

Deletion of the $\beta 4$ Signaling Domain Suppresses ErbB2-Driven Mammary Gland Tumorigenesis

Mice carrying a targeted deletion of the $\beta 4$ signaling domain ($\beta 4^{1355T/1355T}$; see Figure S1 in the Supplemental Data available with this article online) exhibit defects in wound healing and postnatal angiogenesis, consistent with the observation that this mutation does not impair $\alpha 6 \beta 4$ -dependent adhesion or assembly of hemidesmosomes but suppresses $\beta 4$ signaling (Nikolopoulos et al., 2004, 2005). Whole-mount analysis of ductal outgrowth and immunostaining studies suggest that $\beta 4^{1355T/1355T}$ female mice undergo normal mammary gland morphogenesis (Figure S2). In addition, these mice are able to nurse their progeny effectively. These results indicate that loss of $\beta 4$ signaling does not cause obvious defects in mammary gland development.

To examine the role of $\beta 4$ signaling in mammary tumorigenesis, we introduced the $\beta 4$ -1355T mutation in MMTV-

Neu(YD) mice, which progress rapidly from ductal carcinoma in situ to invasive and metastatic carcinoma (Dankort et al., 2001), allowing an examination of the role of $\beta 4$ signaling during tumor progression. MMTV-*Neu*(YD); $\beta 4^{1355T/1355T}$ (henceforth Neu(YD)/ $\beta 4$ -1355T) mice developed palpable tumors significantly later as compared to control MMTV-*Neu*(YD); $\beta 4^{+/+}$ (Neu(YD)/ $\beta 4$ -WT) mice: Median tumor onset was delayed by approximately 50% in $\beta 4$ mutant mice (Figure 1A). Moreover, they displayed significantly fewer tumors as compared to control mice (Figure 1B). Finally, Neu(YD)/ $\beta 4$ -1355T mice exhibited greatly reduced cumulative tumor burden at 17 and 22 weeks of age (Figure 1C). Heterozygous MMTV-*Neu*(YD); $\beta 4^{+/-1355T}$ mice exhibited an intermediate phenotype (Figure 1A; cumulative tumor burden at 22 weeks: $7.1 \text{ g} \pm 2.1 \text{ SD}$, $n = 6$), suggesting that $\beta 4$ signaling is haploinsufficient for mammary tumor onset and growth. Together, these results indicate that deletion of the $\beta 4$ signaling domain inhibits ErbB2-initiated mammary tumorigenesis.

$\beta 4$ Signaling Promotes Tumor Cell Proliferation and Suppresses Apoptosis

Neoplastic cells in mammary intraepithelial neoplasia (MIN) lesions of Neu(YD)/ $\beta 4$ -WT mice had significantly elevated levels of $\beta 4$ as compared to normal luminal cells (Figure S3A). $\beta 4$ was no longer concentrated at the basement-membrane junction but was instead diffusely distributed over the cell surface. The levels of its basement-membrane ligand, laminin-5, were severely reduced. As MIN lesions progressed to invasive carcinomas, laminin-5 became undetectable, but $\beta 4$ remained elevated (Figure S3B). The tumors of Neu(YD)/ $\beta 4$ -1355T mice exhibited a similar upregulation of $\beta 4$ and downregulation of laminin-5. However, mutant $\beta 4$ remained in part concentrated at the basement-membrane junction in MIN lesions of these mice (Figure S3A), suggesting that $\beta 4$ signaling may disrupt epithelial polarity.

Since established tumors of Neu(YD)/ $\beta 4$ -1355T mice grew only at a modestly reduced rate (approximately 70% of control value; see Figure 1G and below) and were vascularized to the same extent as those of control Neu(YD)/ $\beta 4$ -WT mice (Figure S4), we examined whether loss of $\beta 4$ signaling inhibits mammary tumor induction or initial growth. Neu(YD)/ $\beta 4$ -1355T mice exhibited significantly fewer MIN lesions at 13 weeks of age (2.1 ± 2.4 per median longitudinal section, $n = 7$ mice) as compared to Neu(YD)/ $\beta 4$ -WT mice (10.1 ± 6.6 , $n = 8$ mice, $p = 0.01$), indicating that loss of $\beta 4$ signaling inhibits mammary tumor onset and initial growth.

To dissect the mechanism by which loss of $\beta 4$ signaling suppresses mammary tumorigenesis, preneoplastic and MIN lesions were stained with anti-Ki-67. As shown in Figure 1D, activated ErbB2 induced robust epithelial cell proliferation prior to overt morphological transformation in the ducts and lobules of Neu(YD)/ $\beta 4$ -WT mice (age-matched wild-type mice contained only scattered Ki-67⁺ cells). By contrast, cell proliferation was only modestly

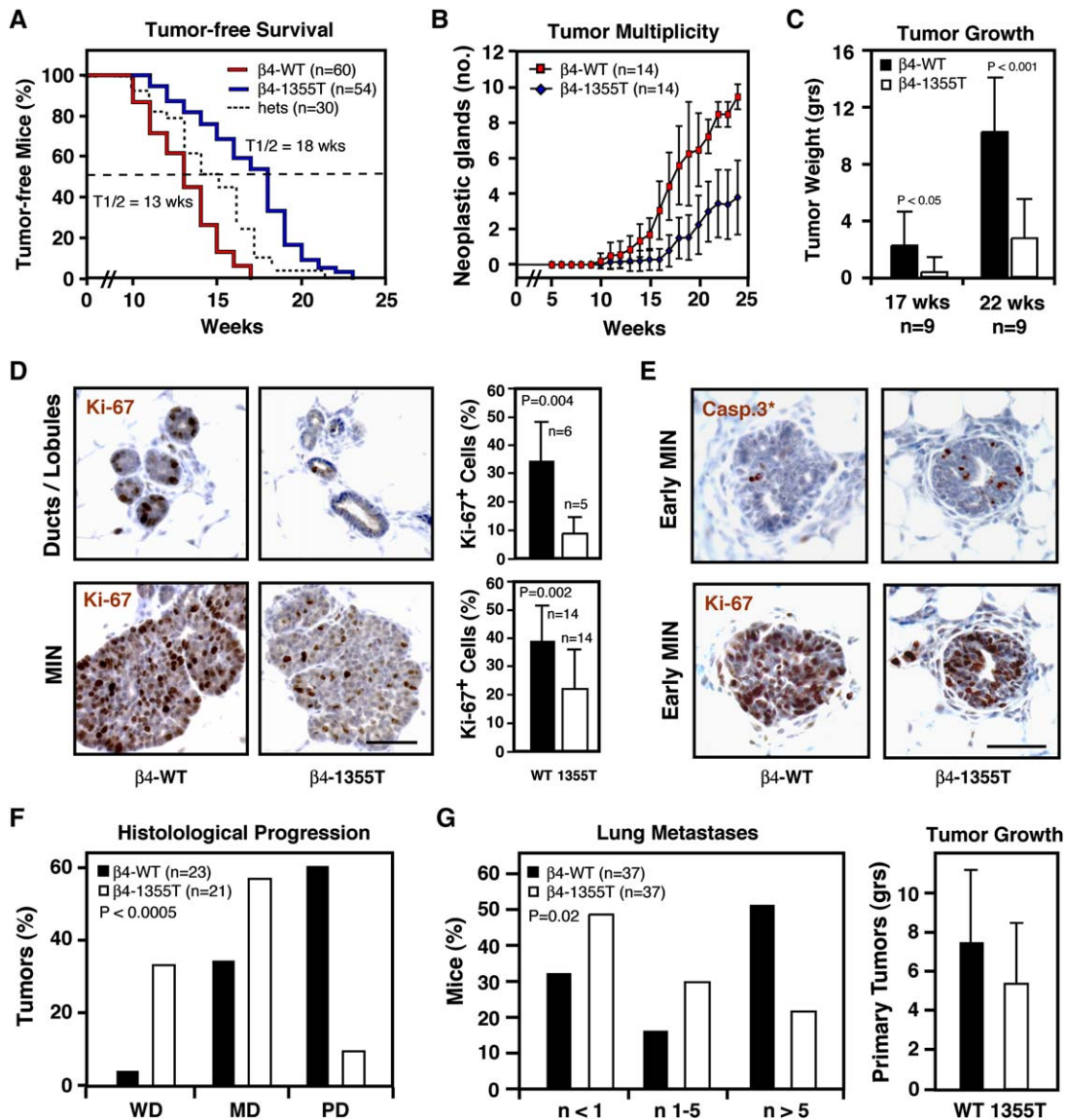


Figure 1. Deletion of the $\beta 4$ Integrin Signaling Domain Suppresses ErbB2-Initiated Mammary Tumorigenesis

(A) Kaplan-Meier analysis of tumor onset. $\beta 4$ -WT versus $\beta 4$ -1355T: $p < 0.0001$ by the log-rank test.

(B) Average number (±SD) of mammary glands containing palpable tumors per mouse per genotype at the indicated ages. After 13 weeks, $p < 0.01$.

(C) Average cumulative tumor burden (±SD) for each cohort at 17 and 22 weeks of age.

(D) Sections of mammary fat pads from 13-week-old mice of the indicated genotype were stained with anti-Ki-67. Representative images of ducts, lobules, and MIN lesions are shown. Scale bar = 50 μm. The graphs show the mean percentage of Ki-67 positive cells (±SD) in ducts and lobules (top, $n =$ mice) and MIN lesions (bottom, $n =$ MIN lesions from four mice).

(E) Consecutive sections of early MIN lesions from 13-week-old mice of the indicated genotype were stained with anti-cleaved caspase-3 (Casp.3*) and anti-Ki-67. Representative images are shown. Scale bar = 50 μm.

(F) Percentages of tumors in each category (WD, well differentiated; MD, moderately differentiated; PD, poorly differentiated) in 5-month-old mice of the indicated genotype.

(G) Mice were sacrificed approximately 7.5 weeks after detection of their first palpable tumor. Sagittal lung sections (2–4 per mouse) were stained with hematoxylin and eosin (H&E) and examined microscopically. The graph on the left shows the percentage of mice of the indicated genotype with <1, 1–5, or >5 metastases per lung section. The graph on the right shows the mean cumulative tumor burden (±SD) in each cohort of mice at the time of euthanasia.

increased in the ducts and lobules of Neu(YD)/ $\beta 4$ -1355T mice. Furthermore, MIN lesions of Neu(YD)/ $\beta 4$ -WT mice contained a significantly higher proportion of proliferating

tumor cells (approximately 40%) than those of Neu(YD)/ $\beta 4$ -1355T mice (approximately 20%) (Figure 1D). Staining with antibodies to cleaved caspase-3 indicated modest

apoptotic rates in most MIN lesions of Neu(YD)/ β 4-WT mice. However, a subset of early MIN lesions with a pervious lumen in Neu(YD)/ β 4-1355T mice contained a significant number of apoptotic cells ($8.9\% \pm 4.4\%$, $n = 4$) (Figure 1E). Interestingly, these lesions had a high proliferative index, suggesting that aberrant cell proliferation contributes to apoptosis in these lesions. By contrast, early MIN lesions with a similarly high proliferative rate in Neu(YD)/ β 4-WT mice exhibited only modest apoptosis ($1.8\% \pm 0.7\%$, $n = 4$, $p = 0.02$) (Figure 1E). These results suggest that β 4 signaling promotes cell proliferation throughout the preneoplastic and the MIN stage and suppresses oncogene-induced apoptosis prior to luminal filling.

Deletion of the β 4 Signaling Domain Inhibits Tumor Progression and Metastasis

ErbB2 mammary tumors progress from MIN to invasive carcinoma through steps characterized by increasing degrees of dedifferentiation (Figure S5A). At 5 months of age, Neu(YD)/ β 4-1355T mice exhibited a high proportion of well-differentiated and moderately differentiated tumors characterized by a glandular appearance. By contrast, Neu(YD)/ β 4-WT mice had developed predominantly poorly differentiated tumors (Figure 1F), suggesting that deletion of the β 4 signaling domain inhibits histological progression. Since mammary tumors of MMTV-Neu(YD) mice primarily metastasize to the lung (Dankort et al., 2001), we examined the lungs of both types of mice 7.5 weeks after primary tumor onset. Most Neu(YD)/ β 4-WT mice had developed a large number of metastases, but many Neu(YD)/ β 4-1355T mice exhibited either no metastases or only a few of them (Figure 1G, left). Cumulative primary tumor burden was similar in the two types of mice (Figure 1G, right). These results suggest that loss of β 4 signaling inhibits tumor invasion and metastasis.

To further examine the effect of β 4 signaling on tumor progression, moderately differentiated tumors from Neu(YD)/ β 4-WT and Neu(YD)/ β 4-1355T mice were stained with antibodies to E-cadherin and the tight-junction component ZO-1. As shown in Figure S5B, both types of tumors retained expression of E-cadherin at the cell surface. However, tumors from Neu(YD)/ β 4-WT mice exhibited severely decreased ZO-1 staining. Tight-junction strands were not apparent, and most of the ZO-1 reactivity was located ectopically in intracellular vesicles. By contrast, tumors from Neu(YD)/ β 4-1355T mice contained clear tight-junction strands between adjacent cells (Figure S5B), suggesting that β 4 signaling promotes disassembly of tight junctions.

β 4 Signaling Disrupts Mammary Epithelial Adhesion and Polarity In Vitro

Tight junctions have emerged as key regulators of mammalian epithelial adhesion and polarity (Macara, 2004). To examine the effect of β 4 signaling on epithelial adhesion and polarity, we isolated primary ErbB2-transformed cells from Neu(YD)/ β 4-WT and Neu(YD)/ β 4-1355T mice and verified that they expressed similar levels of ErbB2 (Figure 2A). Whereas tumor cells expressing wild-type

β 4 exhibited a spindle-like morphology and overlapping margins, those expressing β 4-1355T had polygonal shapes and closely apposed margins. Consistent with their morphology, cells expressing wild-type β 4 had severely disrupted tight junctions and disorganized adherens junctions (Figure 2B). Strikingly, tumor cells expressing β 4-1355T exhibited well-organized cell junctions (Figure 2B), indicating that loss of β 4 signaling restores epithelial adhesion in ErbB2-transformed mammary epithelial cells (MECs). Gefitinib (Iressa), which was developed to block EGF-R but also inhibits ErbB2 with an IC_{50} of approximately $1 \mu M$ (Figure S6A; Moasser et al., 2001), promoted reassembly of adherens and tight junctions in tumor cells expressing wild-type β 4 (Figure 2B). Since ErbB2-transformed MECs do not express detectable levels of EGF-R in vitro (Figure S6B), it is likely that Iressa exerts its effect in these cells by inhibiting ErbB2. These results suggest that the β 4 integrin cooperates with ErbB2 to induce disruption of epithelial adhesion.

Studies of MECs in organotypic 3D Matrigel culture have highlighted the contribution of epithelial adhesion and polarity to growth inhibition (Bissell et al., 2003). As anticipated, tumor cells expressing wild-type β 4 formed expansive solid spheroids in 3D Matrigel (Figure 2C). Immunofluorescence staining showed that these structures were profoundly disorganized. Laminin-5 was deposited both around and inside tumor cell aggregates, and the β 4 integrin was diffusely distributed over the cell surface (Figure 2D). In addition, E-cadherin and β -catenin were not concentrated at adherens junctions (unpublished data), and ZO-1 was present in intracellular vesicles (Figure 2D). In striking contrast, most tumor cells expressing β 4-1355T assembled pseudoacinar structures (Figure 2C). These structures possessed a lumen and exhibited a distinctive epithelial organization and polarity. The mutant integrin was concentrated at the basal cell surface, and laminin-5 was deposited exclusively underneath this surface (Figure 2D). E-cadherin and β -catenin were partially localized at cell-to-cell junctions (unpublished data), and ZO-1 was concentrated in tight-junction strands at the apical junctional complex (Figure 2D). Thus, loss of β 4 signaling restores a significant degree of epithelial polarity to ErbB2-transformed MECs.

To examine the effect of β 4 signaling on growth control, we monitored tumor cell proliferation in 3D Matrigel. Over an 11 day period, the disorganized aggregates consisting of tumor cells expressing wild-type β 4 expanded continuously. By contrast, the pseudoacinar spheroids formed by cells expressing mutant β 4 underwent a very limited expansion (Figure S7), indicating that β 4 signaling is required for ErbB2-induced epithelial hyperproliferation. These results suggest that β 4 signaling contributes to disrupt both epithelial organization and growth control.

The β 4 Integrin Disrupts Epithelial Organization by a Direct Signaling Mechanism

Because β 4 signaling promotes tumor cell proliferation at the MIN stage, it may favor the accumulation of secondary

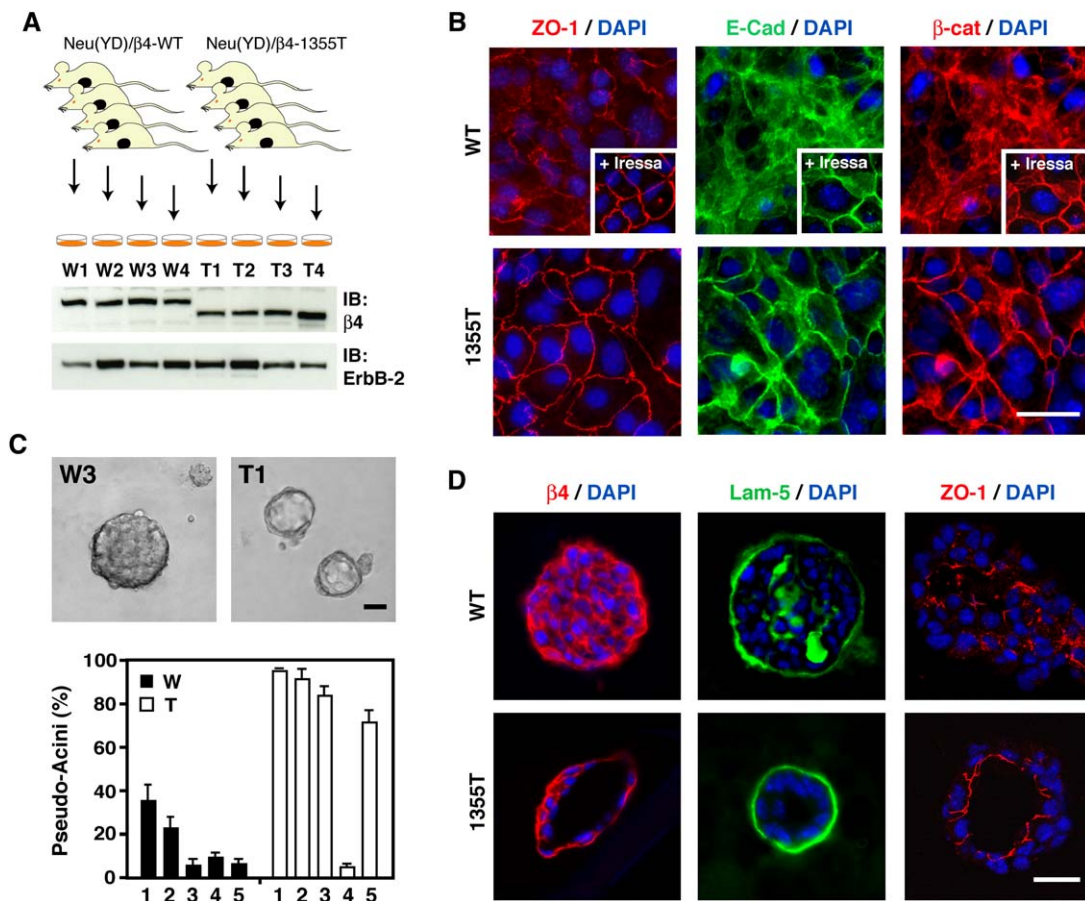


Figure 2. Ex Vivo Analysis of Epithelial Adhesion and Polarity

(A) Four populations of primary Neu(YD)/ β 4-WT (W1–W4) and Neu(YD)/ β 4-1355T (T1–T4) tumor cells were isolated and subjected to immunoblotting with anti- β 4 and anti-ErbB2.

(B) Primary tumor cells ($n = 3$ per genotype) were cultured on collagen I in the presence of 5% FBS overnight and subjected to staining with anti-ZO-1 or double staining with anti-E-cadherin (E-cad) and anti- β -catenin (β -cat) followed by counterstaining with DAPI. The insets show wild-type cells treated overnight with 10 μ M Iressa. Scale bar = 25 μ m.

(C) W1–W5 and T1–T5 cells were cultured in 3D Matrigel in serum-free medium for 13 days. The upper panels show phase-contrast images of W3 and T1 cells. Scale bar = 50 μ m. The graph shows the percentages (\pm SD) of pseudoacini formed by each primary tumor cell population in 3D Matrigel. T4 cells formed solid aggregates in Matrigel. However, Iressa only partially restored cell junctions in these cells (unpublished data), suggesting that they had accumulated genetic lesions able to disrupt cell polarity independently of ErbB2 signaling.

(D) 3D Matrigel cultures ($n = 3$ per genotype) were fixed at day 13, sectioned, and stained as indicated. Scale bar = 50 μ m.

mutations driving tumor progression. To examine whether the β 4 integrin disrupts epithelial adhesion by a direct signaling mechanism, we used an RNAi-reconstitution strategy to generate isogenic Neu-transformed MECs expressing either wild-type or mutant β 4 (Figure 3A). Notably, whereas the Neu- β 4-WT cells failed to organize adherens and tight junctions, the Neu- β 4-1355T cells assembled both types of junctions in culture (Figure S8A). Iressa restored junction formation in Neu- β 4-WT cells (Figure S9C). These results suggest that the β 4 integrin induces disruption of cell junctions by a direct signaling mechanism.

Constitutively active RTKs and SFKs can induce disassembly of adherens junctions through Snail/Slug-mediated repression of *E-cadherin* or tyrosine phosphor-

ylation and endocytosis of the E-cadherin/ β -catenin complex (Thiery, 2002). Studies with inhibitors suggested that ErbB2 disrupts epithelial adhesion in Neu- β 4-WT cells through SFK signaling (Figure S9C), but not through activation of PI-3K or MMP 1, 2, 3, and 9 (unpublished data). We did not, however, detect reduced expression of E-cadherin or β -catenin in Neu- β 4-WT cells. In addition, β -catenin was phosphorylated on tyrosine to similar levels in Neu- β 4-WT and Neu- β 4-1355T cells (Figure S8B). These experiments suggest that β 4 enables ErbB2 to disrupt epithelial adhesion through a novel mechanism.

To examine the effect of β 4 signaling on mammary tumor architecture, Neu- β 4-WT and Neu- β 4-1355T cells were implanted in the mammary fat pad of athymic nude mice. Over a 3 week period, Neu- β 4-WT cells formed

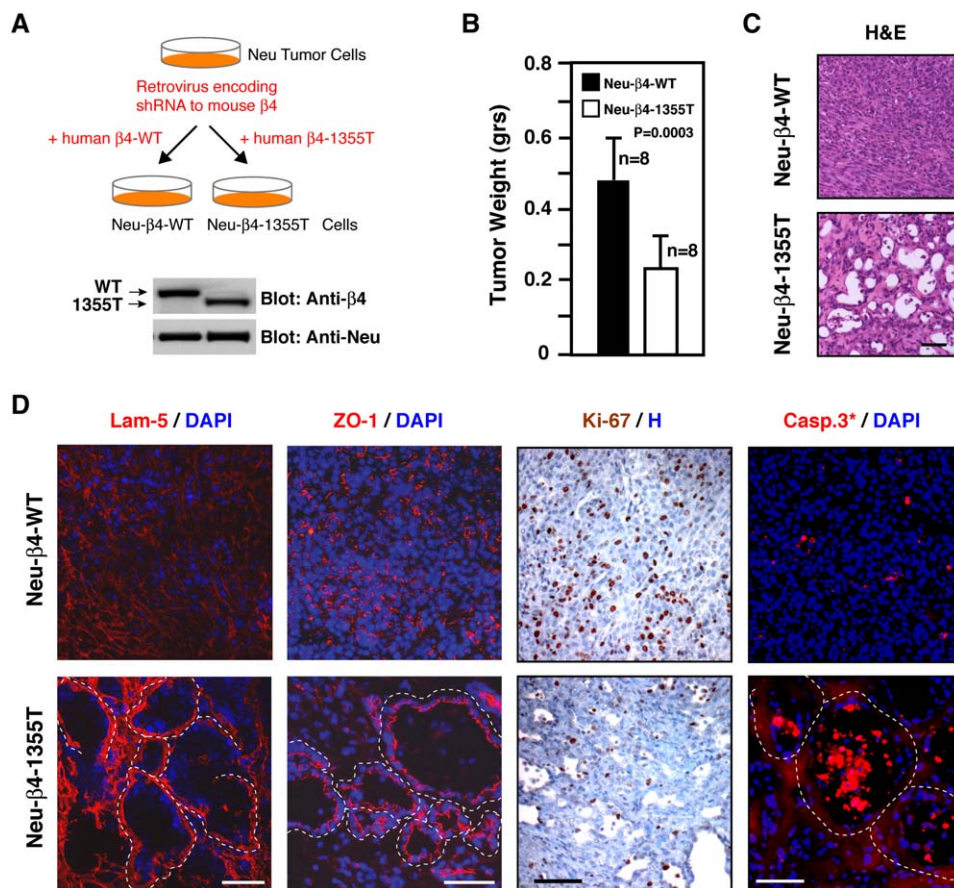


Figure 3. The $\beta 4$ Integrin Disrupts Epithelial Adhesion and Induces Hyperproliferation by a Direct Signaling Mechanism

(A) Primary tumor cells from MMTV-*Neu*(*YD*) mice lost expression of Neu after 3–4 passages in culture and were then rescued with an activated form of ErbB2 (Neu). These cells were then infected with retroviral vectors encoding either human $\beta 4$ -WT or $\beta 4$ -1355T in combination with a shRNA designed to selectively knock down endogenous mouse $\beta 4$. Equal amounts of total proteins were subjected to immunoblotting with anti- $\beta 4$ or anti-ErbB2. (B) Neu- $\beta 4$ -WT and Neu- $\beta 4$ -1355T cells were implanted in the mammary fat pad of athymic nude mice. The graph shows the mean tumor weight \pm SD at day 23.

(C) Orthotopic tumors were sectioned and subjected to H&E staining. Representative pictures are shown ($n = 8$). Scale bar = 50 μ m.

(D) Orthotopic tumors were stained as indicated ($n = 4$). Dotted lines were drawn along the basement membrane of pseudoglandular structures. Scale bars = 50 μ m.

tumors approximately 2-fold larger than those generated by Neu- $\beta 4$ -1355T cells (Figure 3B). Tumors expressing wild-type $\beta 4$ had a solid histological appearance and lacked signs of tissue organization (Figure 3C). Immunofluorescence staining detected scattered, short fibrils of laminin-5 (Figure 3D) and collagen IV (unpublished data). β -catenin was diffusely distributed near the cell surface (unpublished data), and ZO-1 was predominantly present in intracellular vesicles (Figure 3D). By contrast, tumors expressing mutant $\beta 4$ exhibited a striking pseudoglandular organization (Figure 3C). The epithelial cells surrounding the lumens of glandular structures were supported by a continuous, albeit partially disorganized, basement membrane containing laminin-5 (Figure 3D) and collagen IV (unpublished data). They exhibited many seemingly normal β -catenin-containing junctions (unpublished data) and assembled ZO-1-containing tight junctions to-

ward their apical pole (Figure 3D). Staining with antibodies to Ki-67 and to cleaved caspase-3 showed that Neu- $\beta 4$ -1355T tumors contained significantly fewer proliferating cells and more apoptotic cells as compared to Neu- $\beta 4$ -WT tumors (Figure 3D). Notably, the apoptotic cells in Neu- $\beta 4$ -1355T tumors were concentrated in the lumens of pseudoglandular structures, indicating that $\beta 4$ signaling suppresses anoikis. These results illustrate the ability of $\beta 4$ signaling to coordinately disrupt epithelial polarity and growth control in vivo.

$\beta 4$ Signaling Promotes Mammary Tumor Cell Proliferation and Invasion

To further study the effect of $\beta 4$ signaling on ErbB2-mediated proliferation and invasion, we examined the behavior of Neu- $\beta 4$ -WT and Neu- $\beta 4$ -1355T cells in vitro. In the absence of serum, the Neu- $\beta 4$ -1355T cells proliferated

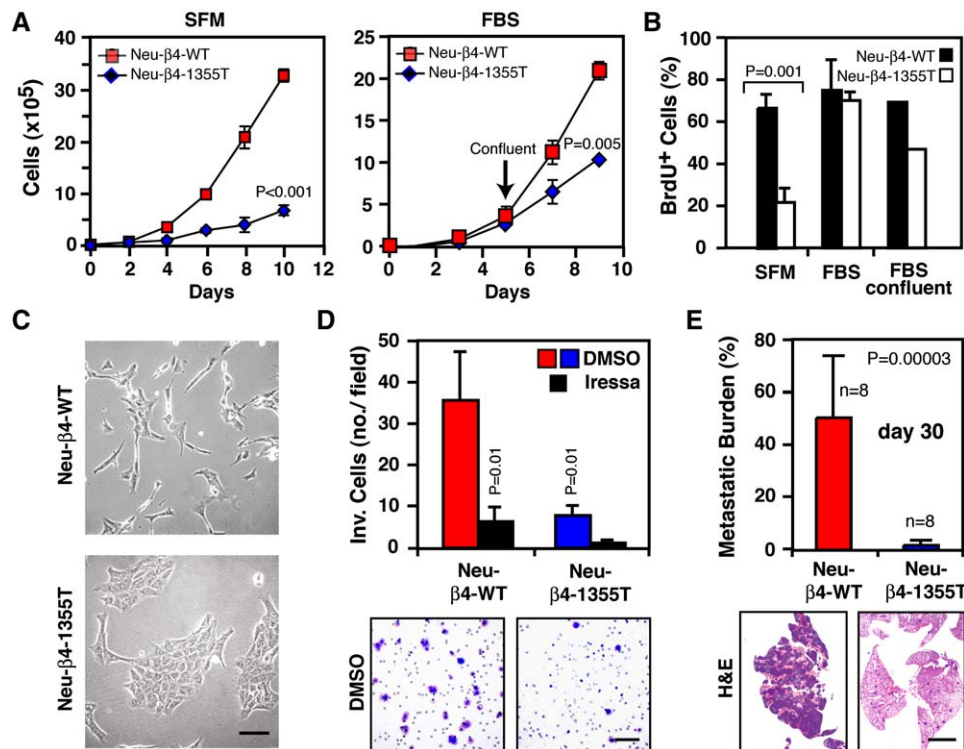


Figure 4. β4 Signaling Promotes Tumor Cell Proliferation, Invasion, and Metastasis

(A) Cells were cultured on collagen I in serum-free medium (SFM) or with 10% FBS. Triplicate samples were counted at the indicated times. Error bars represent SD.

(B) Cells were cultured on collagen I under sparse conditions with SFM or 10% FBS (FBS) or at confluency with 10% FBS (FBS confluent) in the presence of BrdU for 24 or 28 hr, respectively. The graph shows the percentage of BrdU⁺ cells (±SD for SFM and FBS).

(C) Cells were seeded at low density on collagen I and cultured in complete medium for 2 days. Scale bar = 50 μm.

(D) Cells treated with Iressa (10 μM) or vehicle alone (DMSO) were subjected to Matrigel invasion assay in response to FBS. The graph shows the mean number of invaded cells (±SD) per microscopic field from triplicate samples. The bottom panels show representative fields. Scale bar = 50 μm.

(E) Cells were injected in the tail vein of nude mice. Percentages of lung section areas occupied by metastases (±SD) were quantified 30 days later by image analysis. Bottom panels show representative images of sagittal lung sections. Scale bar = 2 mm.

at a dramatically reduced rate in comparison to Neu-β4-WT cells (Figures 4A and 4B). In the presence of serum, both types of cells proliferated at similar rates during the initial phase of growth. However, upon reaching confluency, the Neu-β4-1355T cells proliferated less rapidly as compared to control Neu-β4-WT cells (Figures 4A and 4B). These results suggest that β4 signaling enables activated ErbB2 to promote growth-factor-independent mitogenesis and contributes to a certain extent to its ability to disrupt contact inhibition.

Consistent with their inability to form cell-to-cell junctions, Neu-β4-WT cells scattered extensively in culture. In contrast, the Neu-β4-1355T cells grew as clusters of tightly adhering cells (Figure 4C). When subjected to Matrigel invasion assay, the Neu-β4-WT cells invaded efficiently, and Iressa prevented their invasion. In contrast, the Neu-β4-1355T cells invaded poorly through Matrigel (Figure 4D). Finally, upon intravenous injection in athymic nude mice, Neu-β4-WT cells produced numerous, large metastases in the lung, but Neu-β4-1355T formed only a few micrometastases (Figure 4E). Together with the ob-

servation that Neu(YD)/β4-1355T mice progress to lung metastasis less efficiently than Neu(YD)/β4-WT mice (Figure 1G), these results indicate that β4 signaling promotes mammary tumor invasion and metastasis.

The β4 Integrin Amplifies ErbB2 Signaling

Biochemical studies were performed to examine the molecular mechanism by which β4 signaling promotes mammary tumorigenesis. Coimmunoprecipitation analysis of Neu-β4-WT cells indicated that ErbB2 forms a complex with α6β4 and induces tyrosine phosphorylation of β4 (Figure 5A). Whereas Iressa suppressed tyrosine phosphorylation of both ErbB2 and β4, PP2 suppressed phosphorylation of β4 but only partially inhibited phosphorylation of ErbB2 (Figure 5A), suggesting that ErbB2 induces phosphorylation of β4 through SFKs. Notably, formation of the β4-ErbB2 complex and tyrosine phosphorylation of β4 did not require ligand binding to α6β4 (unpublished data) or the kinase activity of ErbB2 or SFKs (Figure 5A). Comparative coimmunoprecipitation of Neu-β4-WT and Neu-β4-1355T cells revealed that deletion of

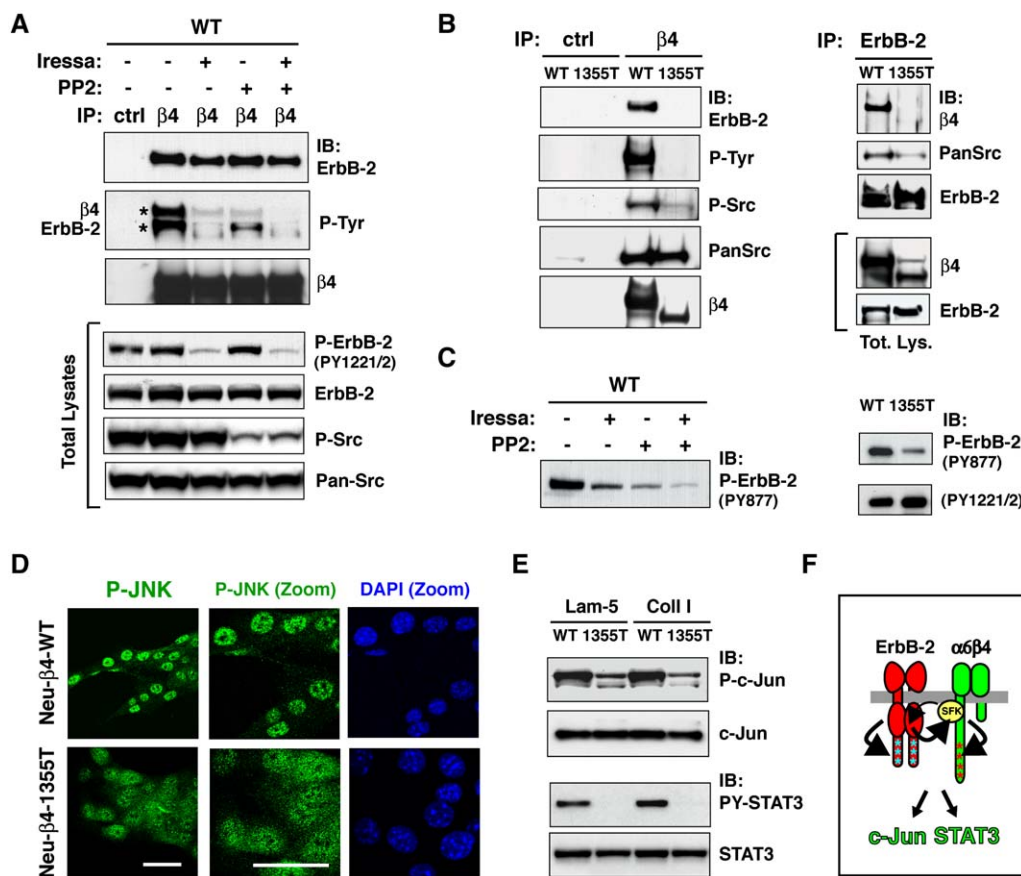


Figure 5. The $\beta 4$ Integrin Associates with ErbB2 and Amplifies Its Signaling Capacity

(A) Neu- $\beta 4$ -WT cells (WT) were cultured on collagen I in SFM and left untreated or treated with Iressa (10 μ M) or PP2 (10 μ M) for 90 min. Equal amounts of total proteins were immunoprecipitated by anti- $\beta 4$ or control anti-MHC I mAb and subjected to immunoblotting with anti-ErbB2, anti-P-Tyr, or anti- $\beta 4$. Total cell lysates containing equal amounts of proteins were subjected to immunoblotting with the indicated antibodies.

(B) Equal amounts of total proteins from the indicated cells were immunoprecipitated with control anti-MHC I mAb (ctrl), anti- $\beta 4$ mAb, or anti-ErbB2 mAb. Samples were subjected to immunoblotting with the indicated antibodies. Total lysates containing equal amounts of proteins were subjected to immunoblotting with anti- $\beta 4$ and anti-ErbB2.

(C) The indicated cells were cultured in SFM and left untreated or treated with Iressa (10 μ M), PP2 (10 μ M), or both compounds for 90 min. Total lysates containing equal amounts of proteins were subjected to immunoblotting with the indicated antibodies.

(D) The indicated cells were cultured on collagen I in SFM and stained with anti-phospho-JNK and DAPI. Scale bars = 25 μ m.

(E) The indicated cells were starved and plated on laminin-5 (Lam-5) or collagen I (Coll I) in SFM for 85 min. Equal amounts of proteins were subjected to immunoblotting with the indicated antibodies.

(F) Model of joint $\beta 4$ -ErbB2 signaling.

the $\beta 4$ signaling domain uncouples $\alpha 6\beta 4$ from ErbB2 and inhibits activation of integrin-associated SFKs. In addition, it reduces the amount of SFKs associated with ErbB2 (Figure 5B). These results indicate that the $\beta 4$ signaling domain is required for assembly of the $\beta 4$ -ErbB2 complex and promotes SFK association with ErbB2.

Since SFKs can phosphorylate Y845 in the P loop of EGF-R (Ishizawa and Parsons, 2004), we examined the effect of SFK inhibition on phosphorylation of the corresponding tyrosine in the P loop of ErbB2. Immunoblotting of total lysates showed that PP2 and Iressa partially inhibit phosphorylation of the P loop of ErbB2 and, when used in combination, completely suppress phosphorylation of this site (Figure 5C). Similar results were obtained upon replac-

ing PP2 with dasatinib, which inhibits SFKs at nanomolar concentrations (Figure S9A). Deletion of the $\beta 4$ signaling domain inhibited phosphorylation of the P loop but not the major autophosphorylation site of ErbB2 (Figure 5C), suggesting that the $\beta 4$ signaling domain contributes to phosphorylation of the P loop of ErbB2 by promoting SFK association with the RTK (see Figure 5F for a model). Thus, $\beta 4$ functions both upstream and downstream of ErbB2, and deletion of the $\beta 4$ signaling domain uncouples $\beta 4$ from ErbB2, suppressing joint signaling.

To confirm the role of SFKs in $\beta 4$ -ErbB2 signaling, Neu- $\beta 4$ -WT cells were treated with dasatinib, which inhibits SFKs and also Abl, or with Gleevec, which inhibits Abl but not SFKs. Dasatinib suppressed tumor cell proliferation

and restored assembly of cell junctions, whereas Gleevec did not exert these effects (Figures S9B and S9C), providing additional evidence that SFKs play a key role in joint $\beta 4$ -ErbB2 signaling.

$\beta 4$ Signaling Controls Activation of c-Jun and STAT3

To examine the effect of $\beta 4$ on downstream signaling, we studied the activation of ERK, JNK, and Akt in Neu- $\beta 4$ -WT and Neu- $\beta 4$ -1355T cells stably adhering to laminin-5 or collagen I. These kinases were found to be activated to similar levels in both types of cells on either substrate (Figure S10). Since $\beta 4$ integrin signaling promotes nuclear translocation of MAP kinases (Nikolopoulos et al., 2005), we monitored nuclear accumulation of activated ERK and JNK in Neu- $\beta 4$ -WT and Neu- $\beta 4$ -1355T cells. Immunofluorescence staining did not reveal significant differences in nuclear accumulation of activated ERK between the two types of cells (unpublished data). However, whereas P-JNK accumulated in the nucleus in Neu- $\beta 4$ -WT cells, it was diffusely distributed in the cytoplasm in Neu- $\beta 4$ -1355T cells (Figure 5D), suggesting that $\beta 4$ signaling controls nuclear translocation of activated JNK. In agreement with this conclusion, phosphorylation of c-Jun at its JNK phosphorylation site, S63, was substantially suppressed in Neu- $\beta 4$ -1355T cells plated on either laminin-5 or collagen I (Figure 5E). In addition, both Iressa and dasatinib inhibited phosphorylation of c-Jun in Neu- $\beta 4$ -WT cells (Figures S9A and S11). These results indicate that $\beta 4$ contributes to ErbB2 signaling by promoting nuclear translocation of JNK and therefore phosphorylation of c-Jun.

Prior studies have linked SFK-mediated phosphorylation of the P loop of ErbB receptors to JAK-STAT signaling (Ishizawa and Parsons, 2004). We therefore examined the effect of deletion of the $\beta 4$ signaling domain on STAT3 activation. Whereas STAT3 was constitutively phosphorylated at its activation site, Y705, in Neu- $\beta 4$ -WT cells plated on laminin-5 or collagen I, phosphorylation of this residue was almost undetectable in Neu- $\beta 4$ -1355T cells on either matrix ligand (Figure 5E). Furthermore, Iressa and dasatinib inhibited phosphorylation of Y705 in Neu- $\beta 4$ -WT cells (Figures S9A and S11). These results indicate that deletion of the $\beta 4$ signaling domain impairs ErbB2-mediated activation of STAT3.

To examine phosphorylation of c-Jun and STAT3 *in vivo*, sections of mammary glands from 13-week-old mice were stained with anti-P-c-Jun and anti-PY-STAT3. Most pre-neoplastic and tumor cells in MIN lesions of Neu(YD)/ $\beta 4$ -WT mice exhibited prominent nuclear staining for activated c-Jun and STAT3. In contrast, only few epithelial cells in similar lesions from Neu(YD)/ $\beta 4$ -1355T mice displayed strong nuclear staining (Figure S12A). Immunoblotting of mammary fat-pad lysates confirmed the reduction of c-Jun phosphorylation in the lesions of Neu(YD)/ $\beta 4$ -1355T mice (Figures S12B and S12C). The phosphorylation of STAT3 in glandular epithelium could not be accurately quantified by immunoblotting because of the prominent activation of STAT3 in stromal cells (Figure S12A). Together, these results indicate that the $\beta 4$ in-

tegrin enables ErbB2 to activate c-Jun and STAT3 (Figure 5F).

c-Jun Is Necessary for Hyperproliferation and STAT-3 for Disruption of Epithelial Adhesion and Invasion

To examine the role of c-Jun during ErbB2-driven mammary tumorigenesis, we used the dominant-negative mutant TAM67, which suppresses breast cancer cell proliferation by interfering with AP-1-dependent transcription (Ludes-Meyers et al., 2001). Neu- $\beta 4$ -WT cells were transduced with a retroviral vector encoding TAM67 or GFP as a control (Figure 6A). Expression of TAM67 inhibited mammary tumor cell proliferation *in vitro* (Figure 6B) and tumorigenicity *in vivo* (Figure 6C). It did not, however, restore assembly of tight or adherens junctions (Figure 6D) or suppress the ability of Neu- $\beta 4$ -WT cells to invade through Matrigel *in vitro* (Figure 6E). These results suggest that c-Jun is necessary for ErbB2-mediated hyperproliferation but not for disruption of epithelial adhesion.

Recent studies have indicated that STAT3 activation is sufficient to transform mammary epithelial cells *in vitro* (Dechow et al., 2004). Expression of the dominant-negative mutant STAT3 β (Caldenhoven et al., 1996) (Figure 6A) did not inhibit mammary tumor cell proliferation *in vitro* (Figure 6B) or tumorigenicity *in vivo* (Figure 6C). However, it restored assembly of tight junctions to a significant extent and formation of adherens junctions partially (Figure 6D). In addition, STAT3 β inhibited Matrigel invasion (Figure 6E) and experimental metastasis (Figure 6F). These results suggest that STAT3 promotes ErbB2-mediated disruption of cell junctions and invasion but not hyperproliferation.

To confirm the effects of dominant-negative constructs, Neu- $\beta 4$ -WT cells were transduced with lentiviral vectors encoding shRNAs targeting c-Jun or STAT3 (Figure S13A). Knockdown of c-Jun suppressed tumor cell hyperproliferation but did not restore assembly of tight junctions. By contrast, knockdown of STAT3 partially restored assembly of tight junctions without affecting proliferative rates (Figures S13B and S13C). Collectively, these data argue that the $\beta 4$ -ErbB2 complex promotes hyperproliferation through activation of c-Jun and disrupts epithelial adhesion largely through activation of STAT3.

Deletion of the $\beta 4$ Signaling Domain Improves the Efficacy of Anti-ErbB2 Therapy

Because of its ability to sustain oncogenic signaling, the $\beta 4$ integrin may promote tumor resistance to anti-ErbB2 targeted therapy. To explore this possibility, we compared the therapeutic efficacy of Iressa in Neu(YD)/ $\beta 4$ -WT and Neu(YD)/ $\beta 4$ -1355T mice. Iressa was chosen because it inhibits rat ErbB2 effectively (Figure S6) and suppresses the proliferation of breast cancer cells overexpressing ErbB2 (Moasser et al., 2001). In addition, although the tumors arising in MMTV-*Neu* mice contain low levels of EGF-R, it does not appear to be activated (Figure S6C), suggesting that Iressa can specifically suppress ErbB2 in these tumors. The humanized anti-ErbB2 mAb Herceptin

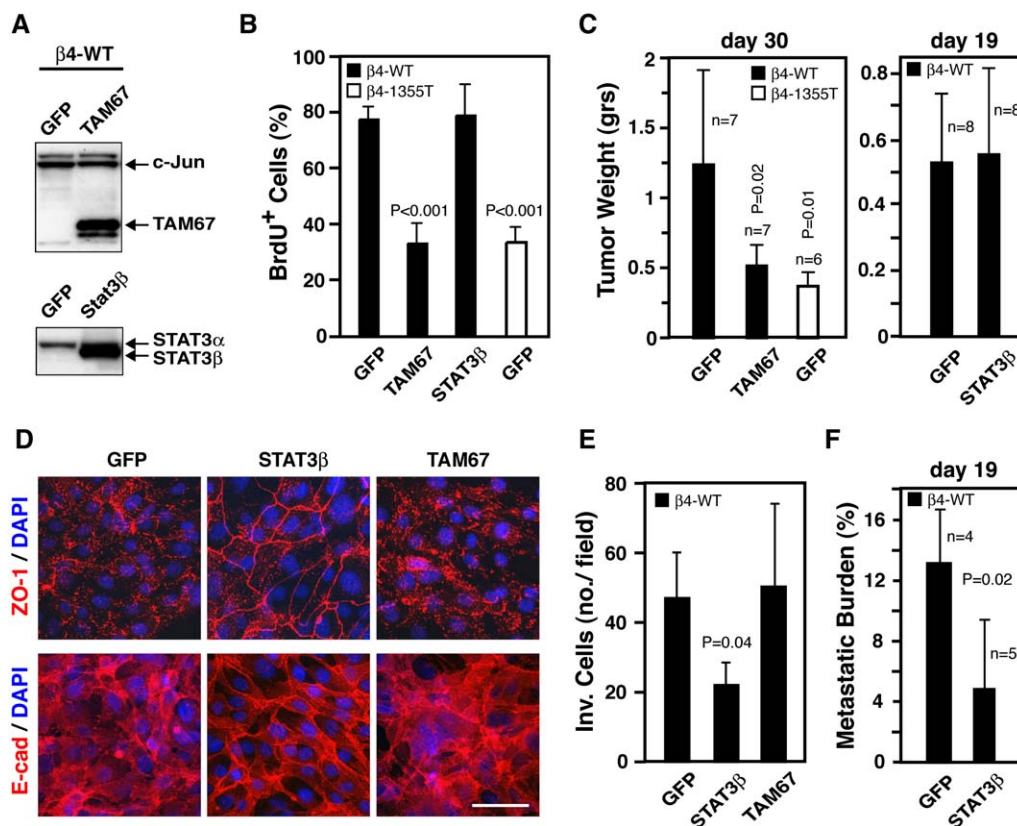


Figure 6. $\beta 4$ Signaling Promotes Tumor Cell Hyperproliferation through c-Jun and Disruption of Epithelial Adhesion and Invasion through STAT3

(A) Neu- $\beta 4$ -WT ($\beta 4$ -WT) cells transduced with retroviral vectors encoding GFP, TAM67, or STAT3 β were subjected to immunoblotting with antibodies reacting with TAM67 and endogenous c-Jun (top) or STAT3 β and endogenous STAT3 α (bottom).

(B) $\beta 4$ -WT cells expressing GFP alone or in combination with TAM67 or STAT3 β and Neu- $\beta 4$ -1355T cells ($\beta 4$ -1355T) expressing GFP alone were cultured on collagen I in serum-free medium containing BrdU for 24 hr. The graph shows the mean percentage \pm SD of GFP-positive BrdU⁺ cells. (C) $\beta 4$ -WT cells expressing GFP alone or in combination with TAM67 or STAT3 β were injected orthotopically in the mammary fat pad, and tumor growth (\pm SD) was evaluated at the indicated times.

(D) $\beta 4$ -WT cells expressing GFP alone or in combination with TAM67 or STAT3 β were cultured on laminin-5 matrix in the presence of 5% FBS. Confluent cultures were stained as indicated. Scale bar = 50 μ m.

(E) $\beta 4$ -WT cells infected with the indicated vectors were subjected to Matrigel invasion assay. The graph shows the mean number of invaded cells per microscopic field (\pm SD).

(F) $\beta 4$ -WT cells infected with the indicated vectors were injected in the tail vein. Lungs were harvested 19 days later, sectioned, and stained with anti-GFP. Percentages (\pm SD) of lung sections occupied by metastases were measured by image analysis.

(trastuzumab) could not be used because it does not react with rat ErbB2.

As shown in Figure 7A, Iressa induced regression of Neu(YD)/ $\beta 4$ -1355T tumors. In contrast, it only reduced the rate of growth of Neu(YD)/ $\beta 4$ -WT tumors (compare with inset). Consistent with its equal apparent IC₅₀ in Neu- $\beta 4$ -WT and Neu- $\beta 4$ -1355T cells in vitro (Figure S6), Iressa suppressed activation of ErbB2 in both types of tumors (Figure 7B). However, whereas the drug inhibited tumor cell proliferation to a significant extent in Neu(YD)/ $\beta 4$ -1355T mice, it exerted a more modest inhibitory effect in Neu(YD)/ $\beta 4$ -WT mice (Figure 7C). In addition, it increased tumor apoptosis in Neu(YD)/ $\beta 4$ -1355T mice to a larger extent than it did in Neu(YD)/ $\beta 4$ -WT mice, although overall apoptotic rates were in both cases very low (<1%).

To examine the specificity of the increased response of Neu(YD)/ $\beta 4$ -1355T tumors to anti-ErbB2 therapy, we treated tumor-bearing Neu(YD)/ $\beta 4$ -WT and Neu(YD)/ $\beta 4$ -1355T mice with the chemotherapeutic drug doxorubicin. Unlike Iressa, doxorubicin reduced the growth rate of tumors in Neu(YD)/ $\beta 4$ -WT and Neu(YD)/ $\beta 4$ -1355T mice to a similar extent, and it failed to induce tumor regression in both types of mice (Figure 7A). These results suggest that $\beta 4$ signaling specifically promotes resistance to anti-ErbB2 therapy.

DISCUSSION

Oncogenic mutations disrupt the regulatory circuits that control cell fate, enabling neoplastic cells to survive and

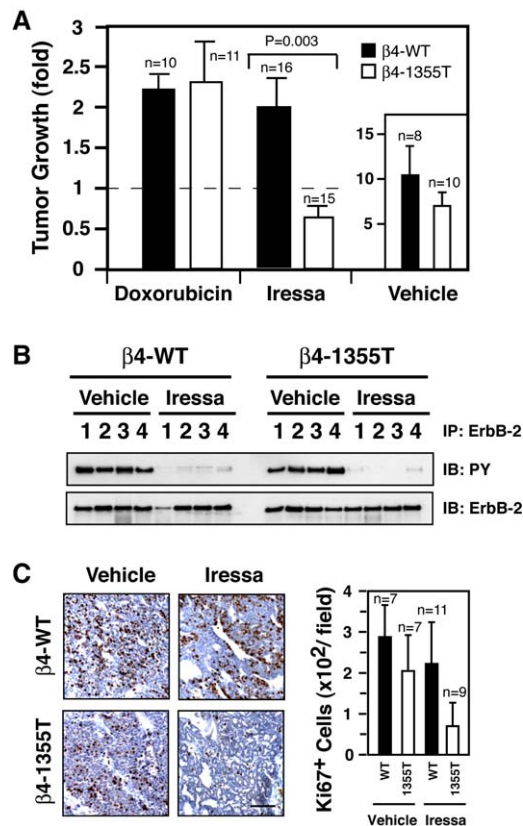


Figure 7. β 4 Signaling Promotes Resistance to anti-ErbB2 Therapy

(A) Tumor-bearing Neu(YD)/ β 4-WT (β 4-WT) and Neu(YD)/ β 4-1355T (β 4-1355T) mice were treated with a single dose of doxorubicin (10 mg/kg) or with Iressa (100 mg/kg/day) or vehicle control (0.1% Tween 80) for 24 days. The graph shows the mean change in tumor volume \pm SEM at day 24 for Iressa or vehicle alone and at day 21 for doxorubicin.

(B) Tumor-bearing mice were treated with Iressa (100 mg/kg/day) or vehicle (0.1% Tween 80) for 9 hr. Equal amounts of total proteins from tumors were immunoprecipitated with anti-ErbB2 and subjected to immunoblotting with anti-P-Tyr (PY) or anti-ErbB2.

(C) Tumor-bearing mice were treated with Iressa (100 mg/kg/day) or vehicle (0.1% Tween 80) for 7 days or more. Tumor sections were stained with anti-Ki-67 followed by counterstaining with hematoxylin. Scale bar = 100 μ m. The graph shows the mean number of Ki-67⁺ cells \pm SD per low-power field. At least four fields were counted (n = tumors).

proliferate at least in part independently of extracellular cues (Hanahan and Weinberg, 2000). It has been intuitively argued that neoplastic cells are no longer dependent on integrin signaling. Our results indicate that β 4 signaling is necessary for tumor cell proliferation and suppression of apoptosis at the onset of ErbB2-initiated mammary tumorigenesis but not for normal mammary ductal outgrowth. This suggests that cancer cells transformed by activated RTKs may be more dependent on specific integrin signals for their proliferation and survival than their normal counterparts. In addition, ablation of all β 1 integrins suppresses polyoma middle T-induced mammary tumor-

igenesis (White et al., 2004), suggesting that integrin signaling is also required for neoplastic conversion of cells transformed by this oncogene. Although additional genetic analyses will be required to fully address the role of integrin signaling in cancer, this evidence indicates that the proneoplastic functions of β 1 integrins and β 4 integrins are not redundant and that two different oncogenes rely on cooperating integrin signals to transform cells.

Our molecular studies indicate that ErbB2 combines with α 6 β 4 and induces sustained phosphorylation of the β 4 signaling domain through activation of SFKs. Conversely, β 4 supports, through its signaling domain, SFK activation and association with ErbB2, thereby controlling phosphorylation of the P loop of ErbB2. These effects seemingly do not require β 4 binding to matrix ligand. Deletion of the β 4 signaling domain uncouples β 4 from ErbB2, disabling SFK-mediated amplification of signaling and activation of c-Jun and STAT3. Thus, β 4 expands ErbB2 signaling, functioning as a cooperating oncogene during ErbB2-mediated mammary tumorigenesis.

The β 4 integrin promotes mammary carcinoma hyperproliferation by inducing phosphorylation and, presumably, activation of c-Jun. The specific mechanisms by which c-Jun participates in oncogenesis are currently debated (Eferl and Wagner, 2003). Knockin of an unphosphorylatable form of c-Jun suppresses formation of skin papillomas in K5-SOS-F mice and colorectal carcinogenesis in *Apc*^{Min} mice (Behrens et al., 2000; Nateri et al., 2005). It does not, however, impair chemical carcinogenesis in the liver, presumably because phosphorylation of c-Jun is not required for suppression of p53-dependent apoptosis (Eferl et al., 2003). Our results link JNK-mediated phosphorylation of c-Jun to oncogenic hyperproliferation in the mammary gland and identify the β 4 integrin as an activator of this process.

Oncogene-induced hyperproliferation causes apoptosis. Several mechanisms operate to overcome this barrier to transformation in mouse models and human tumors (Lowe et al., 2004). Deletion of the β 4 signaling domain induced apoptosis only in MIN lesions undergoing robust hyperproliferation, suggesting that β 4 signaling protects mammary tumor cells from oncogene-induced apoptosis. This prosurvival effect of β 4 was particularly evident in early lesions that had not yet undergone complete luminal filling, suggesting that there is a temporal window during which this mechanism operates. Provocatively, loss of β 4 signaling enabled lumen formation in pseudoacinar structures in Matrigel and caused substantial apoptosis in pseudoglandular structures in orthotopic tumors. Most tumor cells that had lost adhesion to the basement membrane underwent apoptosis under these circumstances, indicating that β 4 signaling contributes to luminal filling also by opposing anoikis. Studies on the HMT-3522 tumor-progression model have linked the prosurvival effect of α 6 β 4 to its ability to promote assembly of hemidesmosomes and epithelial polarity (Weaver et al., 2002) or to mediate laminin-5 signaling in spite of loss of polarity (Zahir et al., 2003). Our data do not exclude that such

mechanisms may operate in breast cancer cells. They suggest nevertheless that, in ErbB2-transformed cells, $\beta 4$ signaling promotes survival despite loss of adhesion to the basal lamina and disruption of polarity.

The $\beta 4$ -ErbB2 complex disrupts epithelial adhesion and promotes invasion in large part through activation of STAT3. Increasing evidence implicates STAT3 in the development of malignancies of the breast and other tissues (Yu and Jove, 2004). Based on the analysis of mouse models of skin cancer and anaplastic lymphoma, it has been proposed that STAT3 contributes to oncogenesis by promoting cell survival and proliferation (Chan et al., 2004; Chiarle et al., 2005). Our results link STAT3 to loss of epithelial adhesion and acquisition of an invasive phenotype. Interestingly, inactivation of STAT3 impairs gastrulation in zebrafish (Yamashita et al., 2002) and epidermal wound healing in mice (Sano et al., 1999), which require that the participant cells undergo partial or complete EMT. The ability of STAT3 to disrupt epithelial adhesion and polarity documented here may explain its role in these morphogenetic processes. Together, this evidence expands the tumorigenic function of STAT3 and suggests that STAT3 participates in both morphogenesis and tumorigenesis by regulating epithelial adhesion and polarity.

Current models suggest that the Par3-Par6 complex and Rho GTPases regulate epithelial polarity by orchestrating the assembly of tight junctions (Macara, 2004). Our results imply that STAT3 activates one or more genes that encode negative regulators of this polarity pathway or of the cellular machinery that executes its program. However, since inhibition of STAT3 induced only partial reassembly of adherens junctions, joint $\beta 4$ -ErbB2 signaling must disrupt adherens junctions through additional mechanisms. In *D. melanogaster*, loss-of-function mutations in the polarity genes *Dlg*, *Scrib*, or *Lgl* are sufficient to elicit invasive tumors similar to human carcinomas (Bilder, 2004). Attempts to separate the growth-suppressive and polarizing function of these genes have failed, suggesting that they suppress proliferation by regulating apicobasal polarity. Our results indicate that the $\beta 4$ -ErbB2 complex disrupts mammary epithelial polarity and growth control through distinct signaling mechanisms and, presumably, transcriptional programs. Similarly, PI-3K controls hyperproliferation and disruption of epithelial polarity through activation of distinct signaling pathways in tumorigenic HMT-3522 MECs (Liu et al., 2004). These observations suggest that the signaling pathways controlling polarity and proliferation have diverged upstream of polarity genes in vertebrates. The existence of separate means to control growth and polarity may have allowed the emergence of independent checkpoints for these two processes, thus preventing disruption of tissue architecture and growth control after a single genetic lesion.

Oncogene-targeted therapies hold great promise in cancer treatment. Trastuzumab, a monoclonal antibody that suppresses ErbB2 signaling, slows progression of ErbB2-positive breast cancers. However, even when combined with standard chemotherapy, this agent is effective

in only about one-third of patients (Slamon et al., 2001). Iressa induced regression of mammary tumors in $\beta 4$ -1355T mice but not in $\beta 4$ -WT mice, although it suppressed ErbB2 kinase activity in both types of mice. These results imply that the $\beta 4$ integrin activates oncogenic signals that promote resistance to anti-ErbB2 therapy. Although future studies are required to elucidate the molecular pathways causing resistance to Iressa in MMTV-*Neu* mice and to determine whether similar mechanisms decrease the sensitivity of human tumors to ErbB2-targeted therapy, this study suggests that monoclonal antibodies or other compounds able to disrupt the $\beta 4$ -ErbB2 complex or $\beta 4$ signaling may inhibit the progression of ErbB2-positive breast carcinoma or increase the effectiveness of current ErbB2-targeted therapies.

EXPERIMENTAL PROCEDURES

Materials and Reagents

See Supplemental Data.

Tumorigenesis Studies

$\beta 4^{1355T/1355T}$ mice were backcrossed five times to FVB/n mice and then bred to FVB/n MMTV-*Neu*(YD) mice (Dankort et al., 2001). *Neu*(YD) lacks four docking sites but retains Y1226 and Y1227, which mediate recruitment of Shc and transformation through both Grb2-dependent and -independent mechanisms (Dankort et al., 2001). Tumorigenesis studies were performed in nulliparous mice from heterozygous crosses between MMTV-*Neu*(YD); $\beta 4^{WT/1355T}$ and $\beta 4^{WT/1355T}$ mice. Tumors were detected by palpation when they reached ~2–3 mm in diameter and were recorded without knowledge of genotype. For orthotopic transplantation, 5×10^6 cells were suspended in 100 μ l of Matrigel diluted 1:1 in PBS and injected into the fat pad of mammary gland number 3. For experimental metastasis, 1×10^6 or 2×10^6 cells were resuspended in 100 μ l PBS and injected into the tail vein. Iressa tablets were dissolved in 0.1% Tween 80 and administered by gastric gavage. Doxorubicin was injected intraperitoneally. Tumor dimensions were measured by caliper.

Immunostaining

Paraffin-embedded sections were subjected to immunohistochemistry with the M.O.M. or VECTASTAIN ABC peroxidase/DAB staining kits (Vector). Cells and frozen sections were fixed with 4% paraformaldehyde for immunofluorescence staining with antibodies to phospho-JNK, E-cadherin, and β -catenin or with methanol or acetone for immunofluorescence staining with antibodies to ZO-1, $\beta 4$, and laminin-5. For BrdU incorporation assays, cells were deprived of serum for 24 hr, cultured in the presence of BrdU for the indicated times, and stained with the BrdU Labeling and Detection Kit (Roche). At least 300 cells per condition were counted.

Cell Culture

Primary tumor cells were dissociated from tumors by incubation with 2.5 mg/ml dispase and collagenase type I (Invitrogen) for 2–4 hr and were then plated on collagen I (20 μ g/ml) in complete medium. These cells lost expression of *Neu*(YD) after three to four passages in culture, presumably as a result of inactivation of the MMTV LTR promoter. To verify that $\beta 4$ also promotes signaling by an activated form of ErbB2 carrying a full complement of cytoplasmic docking sites, these cells were transduced with pWZL-*Neu*8142, which encodes oncogenic rat ErbB2. Hygromycin-resistant cells were then infected with either LTRH1- $\beta 4$ -WT or LTRH1- $\beta 4$ -1355T and sorted by using Dynabeads (DynaL Biotech) coated with the anti- $\beta 4$ mAb 3E1. These tumor cell lines were cultured in complete medium without EGF. For culture in

3D Matrigel, cells were resuspended at 2×10^5 /ml in SFM and diluted 1:1 with Matrigel.

Biochemical Methods

Cells were lysed in RIPA buffer for immunoblotting and in modified RIPA buffer for immunoprecipitation (Supplemental Experimental Procedures). To immunoprecipitate $\beta 4$, lysates containing 4–5 mg proteins were incubated with 20 μ g anti- $\beta 4$ mAb 3E1 or control anti-MHC1 mAb W6.32 conjugated to Sepharose beads (Mariotti et al., 2001). To immunoprecipitate ErbB2, lysates containing 4–5 mg proteins were incubated with 4 μ g anti-rat ErbB2 mAb Ab-9 (NeoMarkers) and 50 μ l Protein G. The beads were washed with modified RIPA buffer without 0.5% DOC prior to SDS-PAGE.

Invasion Assay

Cells (1×10^5) were placed in SFM on Transwell inserts coated with 2 μ g of Matrigel. After incubation in wells containing SFM + 10% FBS for 6 or 7 hr, the inserts were fixed with 4% paraformaldehyde and stained with crystal violet. Experiments were performed in triplicate.

Statistical Analysis

Kaplan-Meier survival curves were analyzed by using Prism 4 (Graph-Pad Software), and p values were calculated using the log-rank test. For assessment of spontaneous metastasis and histological grades, p values were calculated by using the χ^2 test. All other p values were calculated using Student's t test (unpaired, two-tailed).

Supplemental Data

Supplemental Data include Supplemental Experimental Procedures, Supplemental References, and 13 figures and can be found with this article online at <http://www.cell.com/cgi/content/full/126/3/489/DC1/>.

ACKNOWLEDGMENTS

We thank D. Veach for synthesis of dasatinib and Gleevec, M. Sturniolo for experiments with Gleevec, J. Bromberg and P. Siegel for reagents and advice, G. Nolan and T. Sasaki for reagents, the Molecular Cytology Facility of MSKCC for technical help, and members of the Giancotti laboratory for discussions. This work was supported by NIH grants R37 CA58976 (to F.G.G.) and P30 CA08748 (to MSKCC). W.J.M. is supported by a Canada Research Chair in Molecular Oncology. F.G.G. wishes to dedicate this work to the memory of his mother, Marisa Giancotti, and all other women who have succumbed to breast cancer.

Received: November 22, 2005

Revised: April 12, 2006

Accepted: May 30, 2006

Published: August 10, 2006

REFERENCES

- Bachelder, R.E., Marchetti, A., Falcioni, R., Soddu, S., and Mercurio, A.M. (1999). Activation of p53 function in carcinoma cells by the $\alpha 6 \beta 4$ integrin. *J. Biol. Chem.* 274, 20733–20737.
- Behrens, A., Jochum, W., Sibilia, M., and Wagner, E.F. (2000). Oncogenic transformation by Ras and Fos is mediated by c-Jun N-terminal phosphorylation. *Oncogene* 19, 2657–2663.
- Berger, M.S., Locher, G.W., Saurer, S., Gullick, W.J., Waterfield, M.D., Groner, B., and Hynes, N.E. (1988). Correlation of *c-erbB-2* gene amplification and protein expression in human breast carcinoma with nodal status and nuclear grading. *Cancer Res.* 48, 1238–1243.
- Bilder, D. (2004). Epithelial polarity and proliferation control: links from the Drosophila neoplastic tumor suppressors. *Genes Dev.* 18, 1909–1925.

Bissell, M.J., Rizki, A., and Mian, I.S. (2003). Tissue architecture: the ultimate regulator of breast epithelial function. *Curr. Opin. Cell Biol.* 15, 753–762.

Caldenhoven, E., van Dijk, T.B., Solari, R., Armstrong, J., Raaijmakers, J.A., Lammers, J.W., Koenderman, L., and de Groot, R.P. (1996). STAT3 β , a splice variant of transcription factor STAT3, is a dominant negative regulator of transcription. *J. Biol. Chem.* 271, 13221–13227.

Cavallaro, U., and Christofori, G. (2004). Cell adhesion and signalling by cadherins and Ig-CAMs in cancer. *Nat. Rev. Cancer* 4, 118–132.

Chan, K.S., Sano, S., Kiguchi, K., Anders, J., Komazawa, N., Takeda, J., and DiGiovanni, J. (2004). Disruption of Stat3 reveals a critical role in both the initiation and the promotion stages of epithelial carcinogenesis. *J. Clin. Invest.* 114, 720–728.

Chiarle, R., Simmons, W.J., Cai, H., Dhall, G., Zamo, A., Raz, R., Karras, J.G., Levy, D.E., and Inghirami, G. (2005). Stat3 is required for ALK-mediated lymphomagenesis and provides a possible therapeutic target. *Nat. Med.* 11, 623–629.

Dankort, D., Maslikowski, B., Warner, N., Kanno, N., Kim, H., Wang, Z., Moran, M.F., Oshima, R.G., Cardiff, R.D., and Muller, W.J. (2001). Grb2 and Shc adapter proteins play distinct roles in Neu (ErbB-2)-induced mammary tumorigenesis: implications for human breast cancer. *Mol. Cell. Biol.* 21, 1540–1551.

Debnath, J., Mills, K.R., Collins, N.L., Reginato, M.J., Muthuswamy, S.K., and Brugge, J.S. (2002). The role of apoptosis in creating and maintaining luminal space within normal and oncogene-expressing mammary acini. *Cell* 111, 29–40.

Dechow, T.N., Pedranzini, L., Leitch, A., Leslie, K., Gerald, W.L., Linkov, I., and Bromberg, J.F. (2004). Requirement of MMP9 for the transformation of human mammary epithelial cells by Stat3-C. *Proc. Natl. Acad. Sci. USA* 101, 10602–10607.

Eferl, R., and Wagner, E.F. (2003). AP-1: a double-edged sword in tumorigenesis. *Nat. Rev. Cancer* 3, 859–868.

Eferl, R., Ricci, R., Kenner, L., Zenz, R., David, J.P., Rath, M., and Wagner, E.F. (2003). Liver tumor development. c-Jun antagonizes the proapoptotic activity of p53. *Cell* 112, 181–192.

Falcioni, R., Antonini, A., Nistico, P., Di Stefano, S., Crescenzi, M., Natali, P.G., and Sacchi, A. (1997). $\alpha 6 \beta 4$ and $\alpha 6 \beta 1$ integrins associate with ErbB-2 in human carcinoma cell lines. *Exp. Cell Res.* 236, 76–85.

Gamallo, C., Palacios, J., Suarez, A., Pizarro, A., Navarro, P., Quintanilla, M., and Cano, A. (1993). Correlation of E-cadherin expression with differentiation grade and histological type in breast carcinoma. *Am. J. Pathol.* 142, 987–993.

Hanahan, D., and Weinberg, R.A. (2000). The hallmarks of cancer. *Cell* 100, 57–70.

Ishizawa, R., and Parsons, S.J. (2004). c-Src and cooperating partners in human cancer. *Cancer Cell* 6, 209–214.

Liu, H., Radisky, D.C., Wang, F., and Bissell, M.J. (2004). Polarity and proliferation are controlled by distinct signaling pathways downstream of PI3-kinase in breast epithelial tumor cells. *J. Cell Biol.* 164, 603–612.

Lowe, S.W., Cepero, E., and Evan, G. (2004). Intrinsic tumour suppression. *Nature* 432, 307–315.

Ludes-Meyers, J.H., Liu, Y., Munoz-Medellin, D., Hilsenbeck, S.G., and Brown, P.H. (2001). AP-1 blockade inhibits the growth of normal and malignant breast cells. *Oncogene* 20, 2771–2780.

Macara, I.G. (2004). Parsing the polarity code. *Nat. Rev. Mol. Cell Biol.* 5, 220–231.

Mainiero, F., Murgia, C., Wary, K.K., Curatola, A.M., Pepe, A., Blumberg, M., Westwick, J.K., Der, C.J., and Giancotti, F.G. (1997). The coupling of $\alpha 6 \beta 4$ integrin to Ras-MAP kinase pathways mediated by Shc controls keratinocyte proliferation. *EMBO J.* 16, 2365–2375.

Mariotti, A., Kedeshian, P.A., Dans, M., Curatola, A.M., Gagnoux-Palacios, L., and Giancotti, F.G. (2001). EGF-R signaling through Fyn kinase disrupts the function of integrin $\alpha 6 \beta 4$ at hemidesmosomes:

role in epithelial cell migration and carcinoma invasion. *J. Cell Biol.* 155, 447–458.

Moasser, M.M., Basso, A., Averbuch, S.D., and Rosen, N. (2001). The tyrosine kinase inhibitor ZD1839 ("Iressa") inhibits HER2-driven signaling and suppresses the growth of HER2-overexpressing tumor cells. *Cancer Res.* 61, 7184–7188.

Muller, W.J., Sinn, E., Pattengale, P.K., Wallace, R., and Leder, P. (1988). Single-step induction of mammary adenocarcinoma in transgenic mice bearing the activated *c-neu* oncogene. *Cell* 54, 105–115.

Muthuswamy, S.K., Li, D., Lelievre, S., Bissell, M.J., and Brugge, J.S. (2001). ErbB2, but not ErbB1, reinitiates proliferation and induces luminal repopulation in epithelial acini. *Nat. Cell Biol.* 3, 785–792.

Nateri, A.S., Spencer-Dene, B., and Behrens, A. (2005). Interaction of phosphorylated c-Jun with TCF4 regulates intestinal cancer development. *Nature* 437, 281–285.

Nikolopoulos, S.N., Blaikie, P., Yoshioka, T., Guo, W., and Giancotti, F.G. (2004). Integrin $\beta 4$ signaling promotes tumor angiogenesis. *Cancer Cell* 6, 471–483.

Nikolopoulos, S.N., Blaikie, P., Yoshioka, T., Guo, W., Puri, C., Tacchetti, C., and Giancotti, F.G. (2005). Targeted deletion of the integrin $\beta 4$ signaling domain suppresses laminin-5-dependent nuclear entry of mitogen-activated protein kinases and NF- κ B, causing defects in epidermal growth and migration. *Mol. Cell Biol.* 25, 6090–6102.

Parkin, D.M., Bray, F., Ferlay, J., and Pisani, P. (2005). Global cancer statistics, 2002. *CA Cancer J. Clin.* 55, 74–108.

Sano, S., Itami, S., Takeda, K., Tarutani, M., Yamaguchi, Y., Miura, H., Yoshikawa, K., Akira, S., and Takeda, J. (1999). Keratinocyte-specific ablation of Stat3 exhibits impaired skin remodeling, but does not affect skin morphogenesis. *EMBO J.* 18, 4657–4668.

Shaw, L.M., Rabinovitz, I., Wang, H.H., Toker, A., and Mercurio, A.M. (1997). Activation of phosphoinositide 3-OH kinase by the $\alpha 6 \beta 4$ integrin promotes carcinoma invasion. *Cell* 91, 949–960.

Slamon, D.J., Clark, G.M., Wong, S.G., Levin, W.J., Ullrich, A., and McGuire, W.L. (1987). Human breast cancer: correlation of relapse and survival with amplification of the *HER-2/Neu* oncogene. *Science* 235, 177–182.

Slamon, D.J., Leyland-Jones, B., Shak, S., Fuchs, H., Paton, V., Bajamonde, A., Fleming, T., Eiermann, W., Wolter, J., Pegram, M., et al. (2001). Use of chemotherapy plus a monoclonal antibody against HER2 for metastatic breast cancer that overexpresses HER2. *N. Engl. J. Med.* 344, 783–792.

Sorlie, T., Perou, C.M., Tibshirani, R., Aas, T., Geisler, S., Johnsen, H., Hastie, T., Eisen, M.B., van de Rijn, M., Jeffrey, S.S., et al. (2001). Gene expression patterns of breast carcinomas distinguish tumor subclasses with clinical implications. *Proc. Natl. Acad. Sci. USA* 98, 10869–10874.

Thiery, J.P. (2002). Epithelial-mesenchymal transitions in tumour progression. *Nat. Rev. Cancer* 2, 442–454.

Trusolino, L., Bertotti, A., and Comoglio, P.M. (2001). A signaling adapter function for $\alpha 6 \beta 4$ integrin in the control of HGF-dependent invasive growth. *Cell* 107, 643–654.

van de Vijver, M.J., Peterse, J.L., Mooi, W.J., Wisman, P., Lomans, J., Dalesio, O., and Nusse, R. (1988). Neu-protein overexpression in breast cancer. Association with comedo-type ductal carcinoma in situ and limited prognostic value in stage II breast cancer. *N. Engl. J. Med.* 319, 1239–1245.

Weaver, V.M., Petersen, O.W., Wang, F., Larabell, C.A., Briand, P., Damsky, C., and Bissell, M.J. (1997). Reversion of the malignant phenotype of human breast cells in three-dimensional culture and in vivo by integrin blocking antibodies. *J. Cell Biol.* 137, 231–245.

Weaver, V.M., Lelievre, S., Lakins, J.N., Chrenek, M.A., Jones, J.C., Giancotti, F., Werb, Z., and Bissell, M.J. (2002). $\beta 4$ integrin-dependent formation of polarized three-dimensional architecture confers resistance to apoptosis in normal and malignant mammary epithelium. *Cancer Cell* 2, 205–216.

White, D.E., Kurpios, N.A., Zuo, D., Hassell, J.A., Blaess, S., Mueller, U., and Muller, W.J. (2004). Targeted disruption of $\beta 1$ -integrin in a transgenic mouse model of human breast cancer reveals an essential role in mammary tumor induction. *Cancer Cell* 6, 159–170.

Yamashita, S., Miyagi, C., Carmany-Rampey, A., Shimizu, T., Fujii, R., Schier, A.F., and Hirano, T. (2002). Stat3 Controls Cell Movements during Zebrafish Gastrulation. *Dev. Cell* 2, 363–375.

Yang, J., Mani, S.A., Donaher, J.L., Ramaswamy, S., Itzykson, R.A., Come, C., Savagner, P., Gitelman, I., Richardson, A., and Weinberg, R.A. (2004). Twist, a master regulator of morphogenesis, plays an essential role in tumor metastasis. *Cell* 117, 927–939.

Yu, H., and Jove, R. (2004). The STATs of cancer—new molecular targets come of age. *Nat. Rev. Cancer* 4, 97–105.

Zahir, N., Lakins, J.N., Russell, A., Ming, W., Chatterjee, C., Rozenberg, G.I., Marinkovich, M.P., and Weaver, V.M. (2003). Autocrine laminin-5 ligates $\alpha 6 \beta 4$ integrin and activates Rac and NF κ B to mediate anchorage-independent survival of mammary tumors. *J. Cell Biol.* 163, 1397–1407.